Pillar-foundation joint
Edilmatic

GENERAL INFORMATION

The EDILMATIC prefabricated pillar-foundation joint represents an innovative solution for joining prefabricated elements (*Figure 1*).
It ensures, in particular: **continuity in the flexural reinforcements**, easy installation and adjustment which in turn mean **quick assembly** and **limited building** costs.
This joint features components that require installation in the prefabricated elements cast and others that must be assembled on site.
The on-site assembling is dry, only after elements adjustment is finished a grouting with high-performance, self-compacting, self-levelling mortar is made.

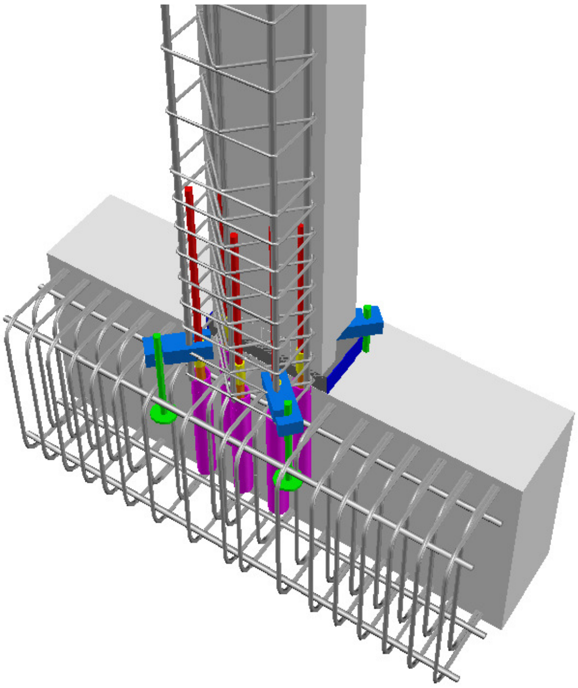

Figure 1. *The Edilmatic pillar-foundation joint*

JOINT COMPONENTS

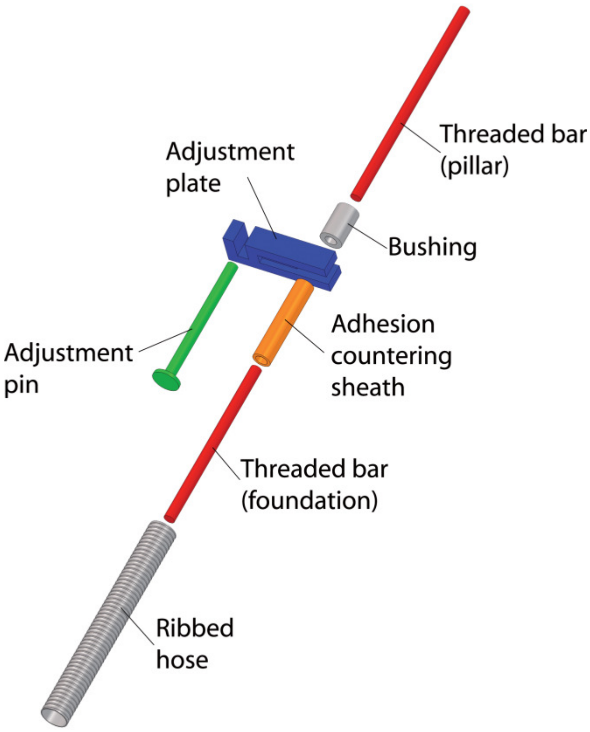

Figure 2. *Joint components description*

The pillar-foundation joint consists of the following elements *(figure 2):*

Pillar casting elements:
- Threaded bars
- Bushings
- Positioning template

Plinth casting elements:
- Ribbed hoses
- Nuts and washers
- Adjustment studs

Assembling and completion components:
- Adjustment plates
- Threaded bars
- Nuts and washers
- Disposable metal formwork for the grouting
- Adhesion countering sheaths
- High-performance mortar

PILLAR CASTING ELEMENTS

Joint components shall be chosen in a way that guarantees equivalence between the calculated moment of resistance using the ordinary reinforcements and the one calculated using the threaded bars.
Every bar is supplied with a *bushing* that shall be installed in the casting via the *positioning template.*
The threaded joint bars are bound to the reinforcement bars of the pillar in a position that allows their placement inside the ribbed hoses inserted in the plinth (*Figure 3*).

Figure 3 *Arrangement / Layout of the threaded joining bars*

Bushings

Table 1 details the sizes of the bushings for every available diameter of the threaded joining bars (*Figure 4*).

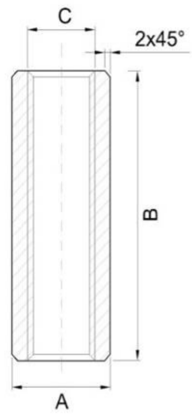

Figure 4

Table 1

	A [mm]	B [mm]	C [mm]
M18	30	55	18
M20	30	60	20
M22	35	70	22
M24	35	75	24
M27	40	85	27
M30	45	90	30
M33	50	100	33
M36	55	110	36

Threaded starter bars

For every available diameter *Table 2* details the required length of the pillar side threaded bars, the Design Strength For Ultimate Limit State (S_{RD}), the yield strength (S_Y) and the ultimate strength (S_U). Minimum length for the threaded starter bar is (*Figure 5*):
$L_{1,min} = 2L_b + B/2$ ...... where: L_b is the anchorage length of a threaded bar, which is 15 times the nominal diameter of the bar (C) and B is the bushing's length.

Table 2

	$L_{1,min}$ [mm]	S_{RD} [kN]	S_y [kN]	S_u [kN]
M18	570	120	138	165
M20	630	153	176	211
M22	700	189	218	261
M24	760	220	254	304
M27	860	286	330	395
M30	950	351	404	482
M33	1040	434	500	597
M36	1140	511	588	703

Figure 5

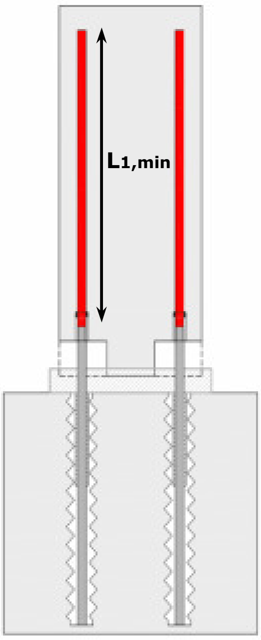

CONNECTION THREADED BARS

the connection is made via threaded bars: one end of the bar is screwed in the bushings fastened to the pillar, the other is inserted in the ribbed hoses of the plinth (*Figure 6*).
Every connection bar is supplied with a PVC sheath, length L_G = 200 mm to nullify the threaded starter bars' bonding capacity while inside the foundation for the purpose of guaranteeing suitable ductility and energy dissipation capacity in case of seismic forces action.
For every available diameter *Table 3* provides length to be used for the connection bars (*Figure 7*).
Minimum length of the connection bars located on the corners is:
$L_{2s,min} = L_b + L_G + B/2 + h_1$
Minimum length of the connection bars in central position is:
$L_{2c} = L_b + L_G + B/2 + h_2$
where:
L_b is the anchorage length of a threaded bar, which is 15 times the nominal diameter of the bar
L_G is the length of the PVC sheaths used to counter and nullify the bars' adhesion (200 mm)
B is the length of the bushing
h_1 is the distance of the base of the pillar from the foundation surface at the corner sockets (recommended value 15 cm)
h_2 is the distance of the base of the pillar from the foundation surface in the central area (recommended value 5 cm)

Figure 6 *Inserting the threaded rods of the pillar in the plinth's ribbed hoses*

Table 3

	$L_{2s,min}$ [mm]	$L_{2c,min}$ [mm]
M18	650	550
M20	680	580
M22	720	620
M24	750	650
M27	800	700
M30	850	750
M33	900	800
M36	950	850

Figure 7

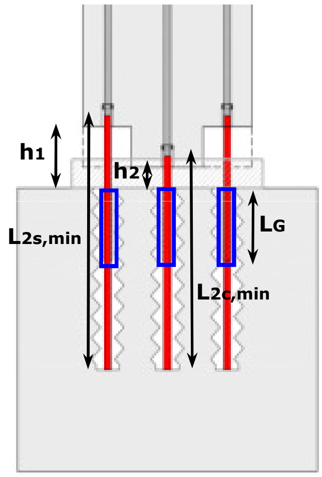

PLINTH CASTING ELEMENTS

During the making of the plinth, make sure to allow for a non-disposable positioning template in the reinforcements' calculation*.* Correct placement of the *threaded started bars* and *ribbed hoses* is obtained by fastening the hoses and the adjustment studs (if any) in the template. The ribbed hoses are then screwed on rubber brackets which are then bolted on the template for the casting (*Figure 8*).
Mounting of the components thus becomes particularly quick ad accurate.

Figure 8 *Positioning the template in the reinforcement cage of the plinth before casting the foundations*

Ribbed hose

The length of the ribbed hose to be laid in the foundations' casting shall be enough to ensure a quick fastening of the threaded connection bars screwed on the pillar bushings.

Table 4 details the geometrical properties of the hoses (diameter D and length $L_{3,min}$) (*Figure 9*).
Minimum length of the ribbed hoses is:
$L_{3,Min} = L_{2c,Min} - h_c + 3cm$
where:
$L_{2c,Min}$ is the anchorage length of the central threaded bars
h_c is the height of the metal formwork is 7 cm

Table 4

	D [mm]	$L_{3,min}$ [mm]
M18	62	510
M20	62	540
M22	62	580
M24	72	610
M27	72	660
M30	72	710
M33	82	760
M36	82	810

Figure 9

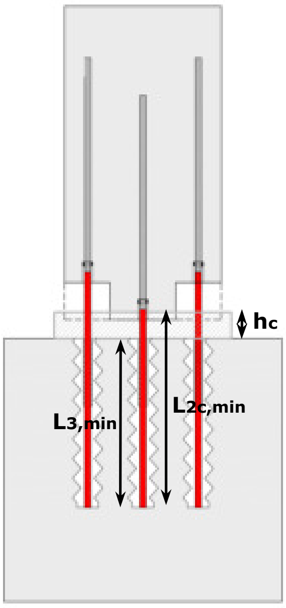

COMPONENTS REQUIRED FOR ASSEMBLING

Adjustment plates

Figure 10 details the elements that compose the system used to adjust the pillar, while *Table 5* details the measurements for each connection bar diameter.

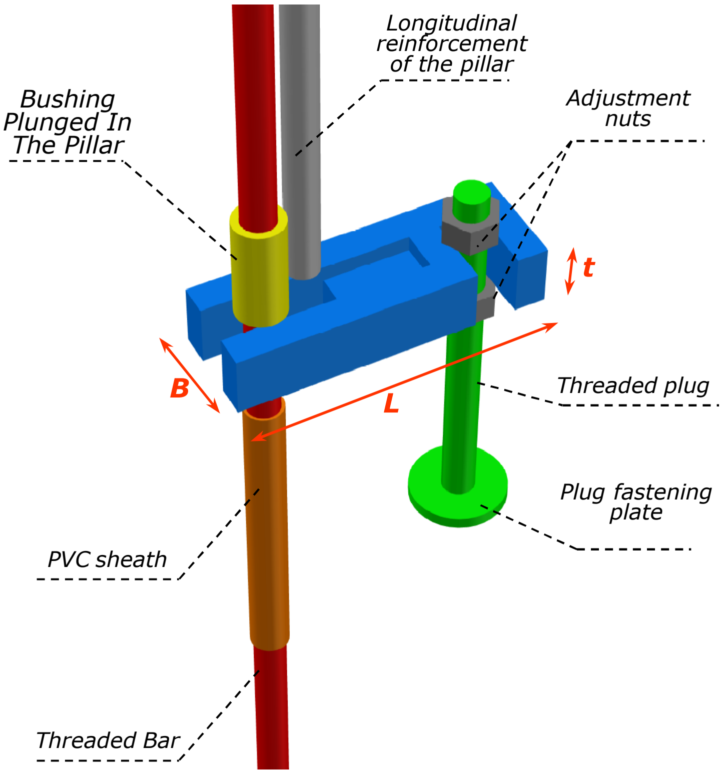

Figure 10 *Pillar adjustment system*

Table 5

	B [mm]	L [mm]	t [mm]
M18÷M20	72	225	50
M22÷M24	76	230	50
M27÷M30	83	250	50
M33÷M36	89	265	50

ASSEMBLING AND COMPLETION

The assembling stage begins by screwing the *threaded connection bars* on the pillar bushings (*Figure 11*).
The connection bars are fastened on the *adjustment plates* that also work as a temporary support for the pillar during the assembling stage; the pillar shall be housed on the *adjustment plates* which in turn are fastened on the *adjustment plugs* buried in the plinth cast (*Figure 12*).
These plugs are sized in a way that ensures a safe support during assembling, guaranteeing that the pillar is stable while the mortar bed sets.
After the dry assembling operations have been completed, lay the modular metal formwork at the base of the pillar. The formwork is a disposable one and works exactly like confinement reinforcement bars (*Figure 13*).

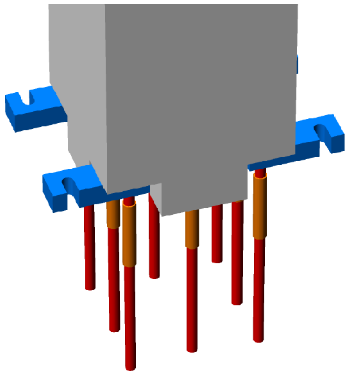

Figure 11 *Step 1*

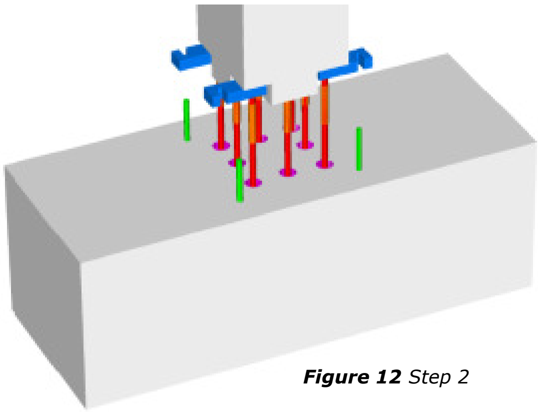

Figure 12 *Step 2*

The next stage is the completion of the joint with an additional cast of high-performance mortar with shrinkage reducing admixture. This additional casting is made in a single step: mortar is poured inside the ribbed hoses until it is level with the metal formwork (*Figure 14*).
After 12 hours have elapsed from the casting, the adjustment corner keys are removed *(Figure 15).*
The pillar sockets will be filled later, upon laying the flooring casting.

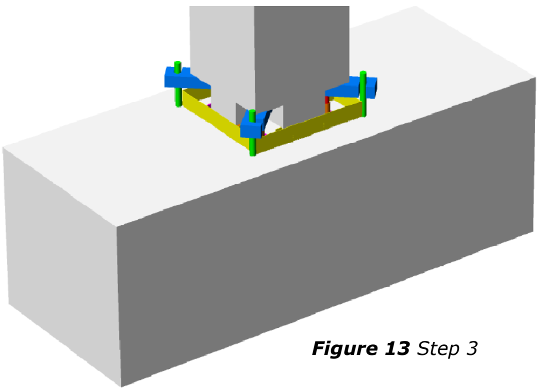

Figure 13 *Step 3*

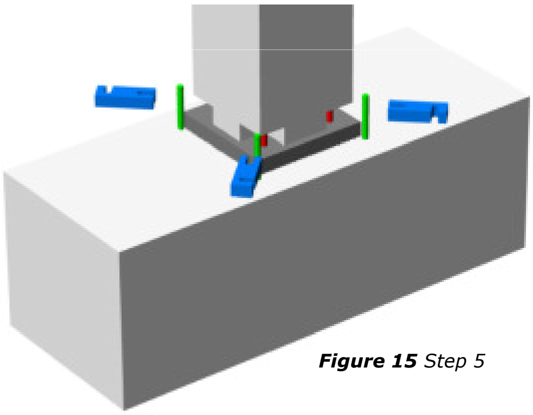

Figure 15 *Step 5*

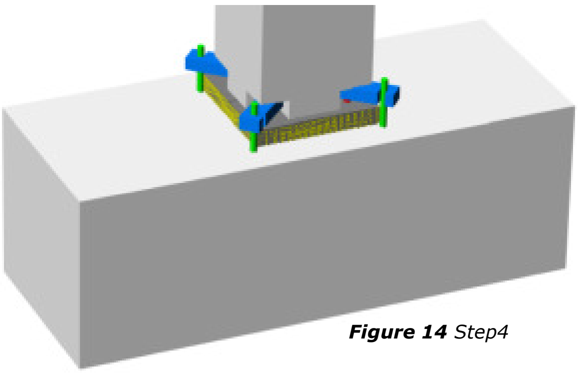

Figure 14 *Step4*

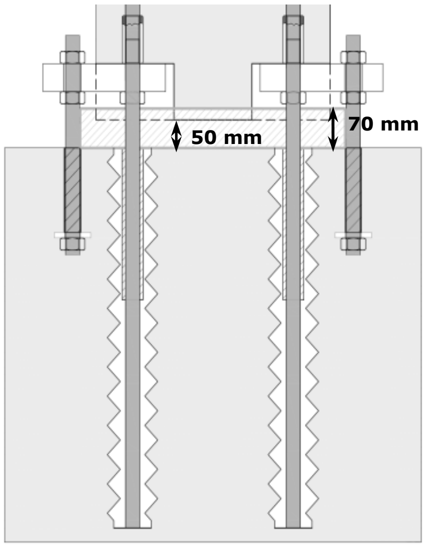

Figure 16 *Pillar height adjustment*

The pillar shall be adjusted so as to make sure that the lower base of the pillar is located at least 2 cm below the upper edge of the metal formwork (*Figure 16*).

EXPERIMENTAL TESTS

The pillar-foundation connection system has undergone a series of experimental tests on full-scale samples; during the tests testers have studied the behaviour of the pillar-foundation joints which were subject to displacement cycles of increasing amplitude. Below we have provided, as an example, the results of the tests carried out on joints built with four threaded starter bars M27 and eight threaded starter bars M18. The behaviour of the joints built with this system has then been compared with a traditional prefabricated plinths with sleeves.

Test bench

Figure 17 describes the test bench elements used for the pillar-foundation joint tests.
The samples have been bound to the ground by anchoring the foundation to the concrete slab of the laboratory by means of two steel sections (**a**) and four pre-tensioned bars. The axial stress is then applied using two jacks (**d**) by means of a system consisting of a steel section laid on the upper head of the pillar (**b**) connected to the foundation by means of two bars, hinged on the bottom (**c**) by means of a steel pin inserted in a hose buried under the foundation casting.
The horizontal stress is instead applied by means of an electromechanical jack anchored to an opposing wall (**e**). The load is applied on the pillar by means of a thrust cap (**f**), consisting of two steel sections which stick on opposing sides of the pillar by means of a system of steel ties; the cap is connected to the head of the jack by means of a series of joints (**g**). The horizontal load application point has been placed about 3.2 metres away from the upper base of the foundation. In order to achieve a better monitoring of the applied force, a load cell (**h**) has been inserted in the system of joints that connects the head of the jack to the pillar.
In order to prevent the test bench from moving or sliding, the foundation has also been bound to the jack's opposing wall by tensioning two bars bound to the steel section (**i**).

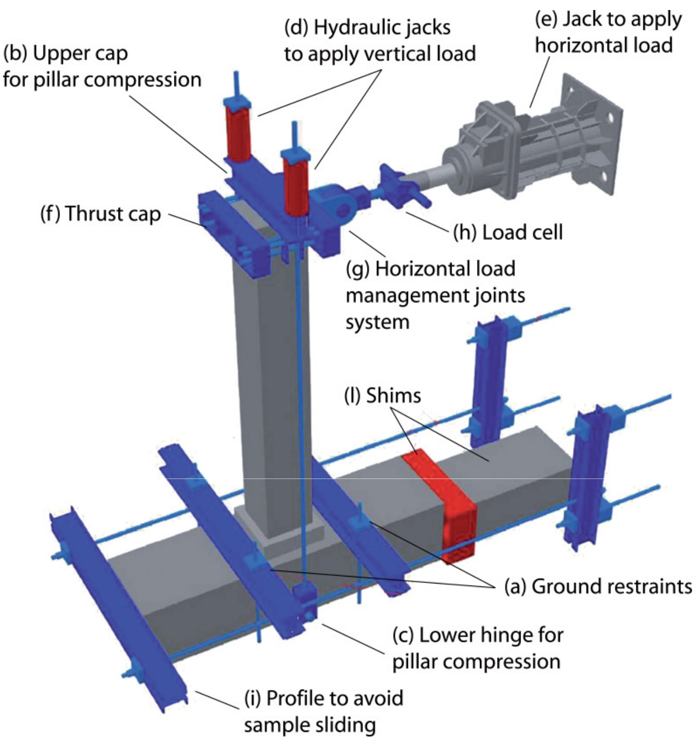

Figure 17 *Test bench*

Load application history

In the first stage a 650 kN axial force has been applied to the test sample. In the next stage the load cycles were gradually increased.
Figure 18 details the various loads applied during the test, in which a horizontal shift δ*x* was applied at the top of the pillar. Subsequently, the test pieces underwent a series of displacement cycles of increasing amplitude, up to a maximum displacement δ*x* of 190 mm, corresponding to a 6% drift.

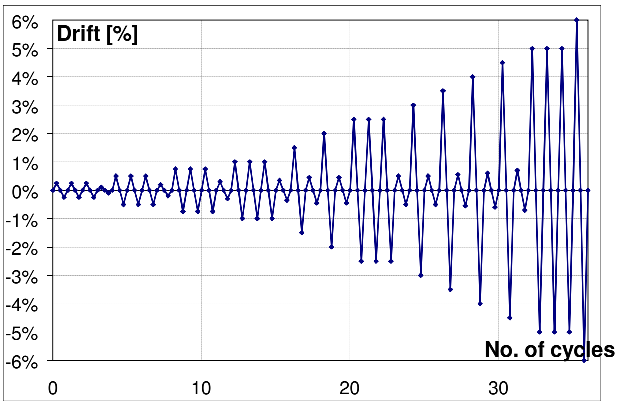

Figure 18 *Load application history*

Experiment results

Moment-drift experimental results are detailed in *Figure 19*, which also features the images of the joint undergoing a 1% and 2.5%, drift, corresponding to a design earthquake with 50% and 10% respective probability of being exceeded in 50 years. Solutions 4 M27 and 8 M18 show an excellent resistance and ductility behaviour up to a 10% drift, corresponding to an actual 190 mm displacement. The tests have been interrupted once this displacement value was reached because the jack's limits (arm length) was reached but samples did not break. Sample 8M18 features a maximum moment of resistance of 327 kNm in the positive cycles and 341 kNm in the negative cycles; those values are slightly lower than the sample 4M27, which features 364 kNm and 381 kNm, respectively (this last value also features an higher arm in the inner torque. The connections' behaviour is stable up to a 2.5% drift which corresponds to a displacement that represents the maximum drift at the design earthquake Ultimate Limit State: when this drift is reached both samples show the maximum moment of resistance.

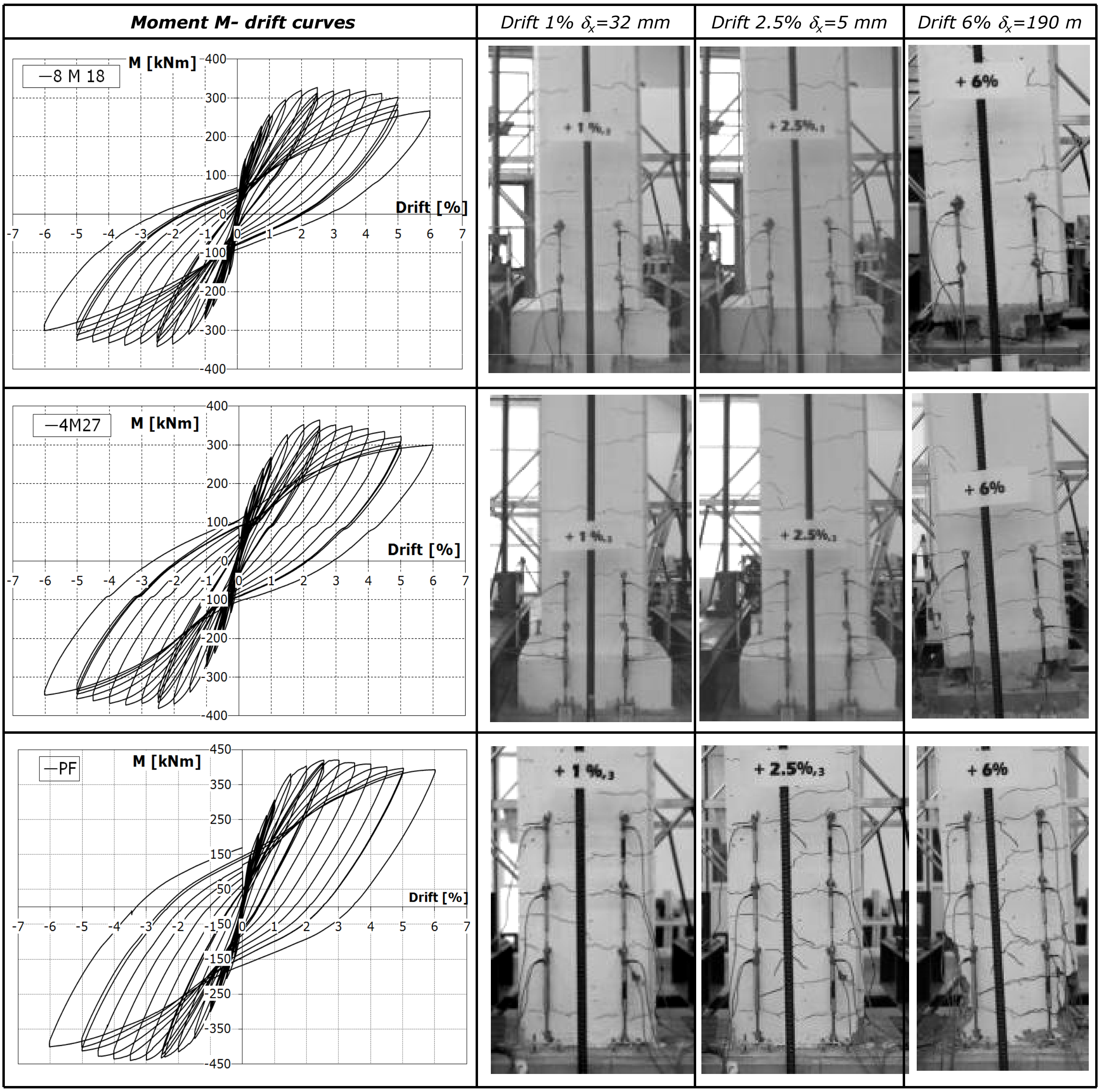

***Figure 19** Experiment results and fissuring behaviour*

'ia Gonzaga, 11 46020 Pegognaga (Mantua) Italy, Phone +39-0376-558225 – fax +39-0376-558672 – E-mail:info@edilmatic.it–internet:www.edilmatic.i

Experiment results

In order to better understand the actual effectiveness of this injected sheathing system it is necessary to compare its effectiveness with the plinth with sleeve systems (PS henceforth). This system features a reduced degradation of joint resistance and a more stable behaviour compared to systems using injected ribbed sheaths for cycles with drift higher than 3%:The joint's moment of resistance is 421 kNm for the positive cycles and 440 kNm for the negative cycles and occurs at drift = 2.5%. When drift reaches 6%, the moment of resistance is is, on average, 91% of the pillar's maximum moment of resistance, compared to 82%and 85% obtained with 4M27 and 8M18 with injected sheaths respectively.
As regards the fissuring behaviour, samples with injected sheaths feature appearance of a small number of cracks along the pillar's height, while maximum damage is found within 20 cm from the base. In heavier cycles the reinforcement cover is expelled and the concrete at the base of the pillar crumbles. As shown in *Figures 20 (a) and (b),* at the end of the test the metal formwork has deformed, which means it has carried out its confinement function and, in addition to that, a through-crack is found in the pillar, namely at the point where the upper edge of the metal formwork where basically the structure switches from full, square section reinforced with high-performance mortar cast to a cross-shaped section in ordinary concrete.
As regards the PS sample, the fissuring behaviour is the one typically found in monolithic structures: several cracks whose length is equal to the pillar size (450 mm), as shown in *Figure 20(c).*

(a) *(b)* *(c)*

Figure 20. *Damages to the samples at the end of the experimental tests: (a) 4 M27; (b) 8 M18; (c) Plinth with sleeve*

Figure 21 shows the graph of the dissipated energy non-dimensionalised with respect to the elastic energy calculated for each cycle; drift values of up to 1% show an almost constant progression. For higher values of drift there is a substantial increase of energy dissipated because of the complete yield of the longitudinal reinforcement bars.
The graph shows that for drifts exceeding 2% the reference sample shows a better behaviour in terms of energy dissipation compared with threaded starter bars but this comes with an increased damage to concrete. when drift reaches 2.5% energy dissipation is 20% higher than the other two samples while when drift reaches 6%, the reference sample's energy dissipation is 12% higher than the 4 M27 sample and 20% higher than the 8 M18 sample.

There is no significant difference between 4M27 and 8M18 for drift values up to 3.5%.
When cycle amplitudes exceed 4% of drift, the 8M18 sample dissipation is 8% lower than the 4M27 sample probably because of the elastic restoring force in the unload stage induced by the two M18 bars placed on the pillar axis.

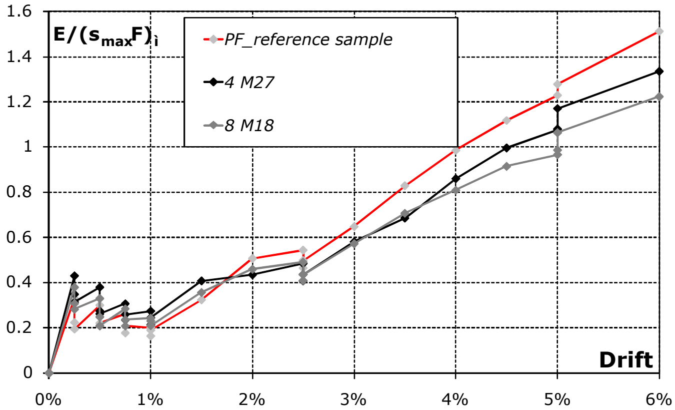

Figure 21. *Non-dimensionalised dissipated energy diagrams*